Multinuclear NMR, Raman, EXAFS, and X-ray Diffraction Studies of Uranyl Carbonate Complexes in Near-Neutral Aqueous Solution. X-ray Structure of [C(NH₂)₃]₆[(UO₂)₃(CO₃)₆]·6.5H₂O

P. G. Allen,[1a,c] J. J. Bucher,[1a] D. L. Clark,*,[1b,c] N. M. Edelstein,*,[1a] S. A. Ekberg,[1b]
J. W. Gohdes,[1b] E. A. Hudson,[1c] N. Kaltsoyannis,[1a] W. W. Lukens,[1a] M. P. Neu,[1b]
P. D. Palmer,[1b] T. Reich,[1d] D. K. Shuh,[1a] C. D. Tait,[1b] and B. D. Zwick[1b]

Chemical Science and Technology Division and Nuclear Materials Technology Division,
Los Alamos National Laboratory, Los Alamos, New Mexico 87545, Chemical Sciences Division,
Lawrence Berkeley Laboratory, Berkeley, California 94720, G. T. Seaborg Institute for Transactinium
Science, Lawrence Livermore National Laboratory, Livermore, California 94551, and
Forschungszentrum Rossendorf e. V., Institut für Radiochemie, Postfach 51 01 19,
D-01314 Dresden, Germany

^{13}C and ^{17}O NMR and Raman spectroscopies were used to monitor the fractions of $UO_2(CO_3)_3^{4-}$ (**1**) and $(UO_2)_3(CO_3)_6^{6-}$ (**2**) in aqueous carbonate solutions as a function of pH, ionic strength, carbonate concentration, uranium concentration, and temperature. The multinuclear NMR and Raman data are consistent with the formation of $(UO_2)_3(CO_3)_6^{6-}$. The pH dependence of the ^{13}C NMR spectra was used to determine the equilibrium constant for the reaction $3UO_2(CO_3)_3^{4-} + 3H^+ \rightleftharpoons (UO_2)_3(CO_3)_6^{6-} + 3HCO_3^-$, log $K = 18.1(\pm0.5)$ at $I_m = 2.5$ m and 25 °C, and corresponds to log $\beta_{36} = 55.6(\pm0.5)$ for the reaction $3UO_2^{2+} + 6CO_3^{2-} \rightleftharpoons (UO_2)_3(CO_3)_6^{6-}$ under the same conditions. Raman spectra showed the uranyl ν_1 stretching band at 831.6 cm^{-1} for monomeric **1** and at 812.5 cm^{-1} for trimeric $(UO_2)_3(CO_3)_6^{6-}$ (**2**). EXAFS data from solid $[C(NH_2)_3]_6[(UO_2)_3(CO_3)_6]$ and a solution of $(UO_2)_3(CO_3)_6^{6-}$ suggest that the same uranium species is present in both the solid and solution states. Fourier transforms of the EXAFS spectra of both solid and solution samples revealed five well-resolved peaks corresponding to nearly identical near-neighbor distances for solid and solution samples of **2**. Fitting of these peaks yields U–O(uranyl) = 1.79, U–O(carbonate) = 2.45, U--C = 2.90, U--O(terminal carbonate) = 4.16, and U--U = 4.91 Å for the solid and similar distances for the solution sample. A peak at 4.75 Å in both Fourier transforms (uncorrected for phase shift) corresponds to a U--U interaction at 4.91 Å, a conclusion which is supported by the absence of this peak in the Fourier transform of the crystalline monomeric $K_4[UO_2(CO_3)_3]$. Multiple scattering along the uranyl vector is believed to play a significant role in the EXAFS of all three systems. The EXAFS data are consistent with the trimeric uranyl carbonate species indicated by NMR spectroscopy. Single crystals of $[C(NH_2)_3]_6[(UO_2)_3(CO_3)_6]·6.5H_2O$ were obtained from a solution that contained stoichiometric amounts of uranyl nitrate and guanidinium carbonate and an excess of guanidinium nitrate at pH 6.5 under a CO₂ atmosphere. The solid state molecular structure of $[C(NH_2)_3]_6[(UO_2)_3(CO_3)_6]·6.5H_2O$ contains a planar D_{3h} trimetallic $(UO_2)_3(CO_3)_6^{6-}$ anion, the structure that Åberg and co-workers originally proposed for the trimeric solution species. The trimetallic anion contains three uranium atoms and all six carbonate ligands in the molecular plane with three uranyl oxygen atoms above and three below the plane. Uranyl U=O distances average 1.78(1) Å, while U–O distances to the carbonate oxygen atoms average 2.41(1) Å for terminal and 2.48(1) Å for bridging ligands. Particularly significant is the average nonbonding U--U distance of 4.97 Å which compares favorably to the 4.91 Å distance seen in the EXAFS analysis. The molecule crystallizes in the triclinic space group $P\bar{1}$, with $a = 6.941(2)$ Å, $b = 14.488(2)$ Å, $c = 22.374(2)$ Å, $\alpha = 95.63(2)°$, $\beta = 98.47(2)°$, $\gamma = 101.88(2)°$, $R = 0.0555$, $R_w = 0.0607$, $V = 2158.5$ Å³, $d_{calc} = 2.551$ g cm^{-3}, and $Z = 2$.

Introduction

Carbonate and bicarbonate are common anions found in significant concentrations in many natural waters and are exceptionally strong complexation agents for actinide ions.[2–5] Therefore, carbonate complexation may play an important role in migration of actinide ions from a nuclear waste repository or in accidental site contamination.[6,7] The stability of actinide carbonate complexes is reflected in the formation of naturally-occurring uranyl carbonate minerals such as rutherfordine, UO_2-(CO_3),[8] leibigite, $Ca_2[UO_2(CO_3)_3]·10-11H_2O$,[9] and andersonite, $Na_2Ca[UO_2(CO_3)_3]·6H_2O$.[10]

⊗ Abstract published in *Advance ACS Abstracts*, August 15, 1995.
(1) (a) Lawrence Berkeley National Laboratory, Mail Stop 70A-1150. (b) Los Alamos National Laboratory, Mail Stop G739. (c) Glenn T. Seaborg Institute. (d) Institute für Radiochemie.
(2) Choppin, G. R.; Stout, B. E. *Sci. Tot. Environ.* **1989**, *83*, 203.
(3) Choppin, G. R.; Allard, B. In *Handbook of the Chemistry and Physics of the Actinides*; Freeman, A. J., Keller, C., Eds.; Elsevier: Amsterdam, 1985; Vol. 3, Chapter 11.
(4) Nash, K. L.; Cleveland, J. M.; Rees, T. F. *J. Environ. Radioactivity* **1988**, *7*, 131.
(5) Kim, J. I. In *Handbook of the Chemistry and Physics of the Actinides*; Freeman, A. J., Keller, C., Eds.; Elsevier: Amsterdam, 1986; Vol. 4, Chapter 8.
(6) Hobart, D. E. *Proc. Robert A. Welch Found. Conf. Chem. Res.* **1990**, *34*, 379.
(7) Grenthe, I.; Lemire, R. J.; Muller, A. B.; Nguyen-Trung, C.; Wanner, H. *Chemical Thermodynamics of Uranium*; OEDC-NEA: Paris, 1991.
(8) Christ, C. L.; Clark, J. R.; Evans, H. T., Jr. *Science* **1955**, *121*, 472.
(9) Apelman, D. *Geol. Soc. Am. Bull.* **1956**, *67*, 1666.
(10) Coda, A.; Della Giusta, A.; Tazzoli, V. *Acta Crystallogr.* **1981**, *B37*, 1496.

Actinide carbonate systems can be quite complicated because several different complex ions can exist in rapid equilibria with one another and with the uncomplexed ion or hydrolyzed species. The uranyl carbonate system is by far the most extensively studied of all actinide carbonate systems.[11-28] The composition and molecular structure of the tris(carbonato) complex of formula $AnO_2(CO_3)_3^{4-}$ is well-established for the light actinides U, Np, Pu, and Am.[10,17,21,29-36] For bis-(carbonato) complexes of empirical formula $AnO_2(CO_3)_2^{2-}$, a trimeric species of composition $[AnO_2(CO_3)_2]_3^{6-}$ has been reported for An = U, Np, and Pu.[17,19,37] For uranyl, this trimer is strongly stabilized in solutions of high ionic strength and is thought to be responsible for the very high solubility of AnO_2-CO_3(s) in carbonate solutions and thus may be important in aquatic transport of actinyl ions via carbonate complexation. The molecular structure of the monomeric $UO_2(CO_3)_3^{4-}$, based on single-crystal X-ray diffraction, is shown schematically in **1**.[10]

1   **2**
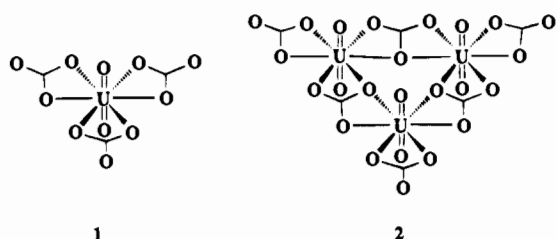
Ciavatta *et al.* were the first to propose the presence of $(UO_2)_3(CO_3)_6^{6-}$ to model potentiometric (emf) titration data.[17] Åberg et al. reported two ^{13}C NMR resonances consistent

(11) Blake, C. A.; Coleman, C. F.; Brown, K. B.; Hill, D. G.; Lowrie, R. S.; Schmitt, J. M. *J. Am. Chem. Soc.* **1956**, *78*, 5978.
(12) Paramonova, V. I.; Nikol'skii, B. P.; Nikolaeva, N. M. *Russ. J. Inorg. Chem.* **1962**, *7*, 528.
(13) Sergeyeva, E. I.; Nikitin, A. A.; Khodakovsky, I. L.; Naumov, G. B. *Geochim. Int.* **1972**, *11*, 900.
(14) Almagro, V.; Garcia, F. S.; Sancho, J. *An. Quim.* **1973**, *69*, 709.
(15) Cinnéide, S. O.; Scanlan, J. P.; Hynes, M. J. *J. Inorg. Nucl. Chem.* **1975**, *37*, 1013.
(16) Nikolaeva, N. M. *Izv. Sib. Otd. Akad. Nauk SSSR* **1976**, *6*, 30.
(17) Ciavatta, L.; Ferri, D.; Grimaldi, M.; Palombari, R.; Salvatore, F. *J. Inorg. Nucl. Chem.* **1979**, *41*, 1175.
(18) Maya, L.; Begun, G. M. *J. Inorg. Nucl. Chem.* **1981**, *43*, 2827.
(19) Ferri, G.; Grenthe, I.; Salvatore, F. *Acta Chem. Scand.* **1981**, *A35*, 165.
(20) Maya, L. *Inorg. Chem.* **1982**, *21*, 2895.
(21) Grenthe, I.; Ferri, D.; Salvatore, F.; Riccio, G. *J. Chem. Soc., Dalton Trans.* **1984**, 2439.
(22) Grenthe, I.; Lagerman, B. *Acta Chem. Scand.* **1991**, *45*, 122.
(23) Ullman, W. J.; Schreiner, F. *Radiochim. Acta* **1988**, *43*, 37.
(24) Ciavatta, L.; Ferri, D.; Grenthe, I.; Salvatore, F. *Inorg. Chem.* **1981**, *20*, 463.
(25) Åberg, M.; Ferri, D.; Glaser, J.; Grenthe, I. *Inorg. Chem.* **1983**, *22*, 3981.
(26) Stout, B. E.; Choppin, G. R.; Sullivan, J. C. In *Transuranium Elements, A Half Century*; Morss, L. R., Fuger, J., Eds.; American Chemical Society: Washington, DC, 1992; p 225.
(27) Brücher, E.; Glaser, J.; Toth, I. *Inorg. Chem.* **1991**, *30*, 2239.
(28) Strom, E. T.; Woessner, D. E.; Smith, W. B. *J. Am. Chem. Soc.* **1981**, *103*, 1255.
(29) Graziani, R.; Bombieri, G.; Forsellini, E. *J. Chem. Soc., Dalton Trans.* **1972**, *19*, 2059.
(30) Mereiter, K. *Acta Crystallogr.* **1988**, *C44*, 1175.
(31) Simakin, G. A. *Radiokhimiya* **1977**, *19*, 424.
(32) Maya, L. *Inorg. Chem.* **1984**, *23*, 3926.
(33) Marquart, R.; Hoffmann, G.; Weigel, F. *J. Less-Common Met.* **1983**, *91*, 119.
(34) Madic, C.; Hobart, D. E.; Begun, G. M. *Inorg. Chem.* **1983**, *22*, 1494.
(35) Basile, L. J.; Ferraro, J. R.; Mitchell, M. L.; Sullivan, J. C. *Appl. Spectrosc.* **1978**, *32*, 535.
(36) Nguyen-Trung, C.; Begun, G. M.; Palmer, D. A. *Inorg. Chem.* **1992**, *31*, 5280.
(37) Grenthe, I.; Riglet, C.; Vitorge, P. *Inorg. Chem.* **1986**, *25*, 1679.

with the structure proposed in **2**.[25] Several years later, Åberg *et al.* used X-ray scattering data from a solution concentrated in the $(UO_2)_3(CO_3)_6^{6-}$ cluster to propose the structural unit shown in **2**.[25] Subsequently, Ferri *et al.* reported five ^{17}O NMR signals for $(UO_2)_3(CO_3)_6^{6-}$ between δ 1130 and 1095 ppm in the expected 2:2:2:1:1 ratio.[38] However, we note that all five [17]O resonances reported for $(UO_2)_3(CO_3)_6^{6-}$ appear in the uranyl (O=U=O) chemical shift region of the ^{17}O NMR spectrum. Since carbonate oxygen signals should appear near 200 ppm in the spectrum,[39] the signals reported by Ferri *et al.* cannot be due to the five types of oxygen present in the proposed trimer structure. Either there were multiple uranyl-containing species present in solution or the structure of the trimer is more complex than originally proposed. These observations prompted the present multinuclear NMR, Raman, EXAFS, and single-crystal X-ray diffraction study of the uranyl carbonate system.

Results and Discussion

In this paper, pH refers to the negative log of an approximate activity of the H^+ ion based on the reading of a pH meter calibrated using commercial buffers. We use p[H] to mean the negative log of the H^+ concentration using a pH meter calibrated with solutions of appropriate ionic strength and known hydrogen ion concentration, as described in the Experimental Section.

Spectroscopic Characterization. ^{13}C NMR. The uranyl carbonate system was studied using ^{13}C NMR spectroscopy of ^{13}C-enriched $UO_2(CO_3)_3^{4-}$ at 0.2 and 0.05 M concentrations and ionic strengths of 4.0 and 2.5 m. Initial solutions were prepared with a carbonate-to-metal ratio of 3:1 in order to favor the formation of the monomeric $UO_2(CO_3)_3^{4-}$ complex (**1**).[7] Careful titration with $HClO_4$ leads to protonation of the carbonate ligand resulting in a decrease in the carbonate:uranyl ratio to 2:1 as proposed by Ciavatta *et al.* and outlined in eq 1.[17,25]

$$3UO_2(CO_3)_3^{4-} + 6H^+ \rightleftharpoons$$
$$(UO_2)_3(CO_3)_6^{6-} + 3CO_2 + 3H_2O \quad (1)$$
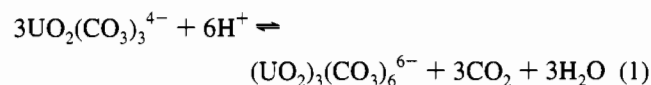
Aliquots were removed at various stages of the titration, flame-sealed in glass NMR tubes, and allowed to equilibrate for approximately 48−72 h. The ^{13}C NMR spectra were recorded at 0 and 23 °C, and a representative series (0 °C) is shown in Figure 1. The longitudinal relaxation rate (T_1) was measured using the inversion recovery method to be 35.9 s, and a 180 s ($5T_1$) pre-acquisition delay was used to obtain accurate integration data. Chemical shifts show small variations with solution conditions (concentration, temperature), and the ambient temperature spectral behavior is consistent with observations reported by others.[25-28] The monomeric $UO_2(CO_3)_3^{4-}$ (**1**) has only one type of carbonate ligand environment and gives rise to a single ^{13}C NMR resonance as seen in Figure 1 at pH 7.92. Upon lowering of the pH, this resonance begins to disappear, and two new resonances of a new species grow in (Figure 1). The proposed structure for $(UO_2)_3(CO_3)_6^{6-}$ (**2**)[24,25] has two inequivalent carbonate ligand environments and should give rise to two, equal-intensity resonances as seen in Figure 1 for the new species that predominates in solution at pH 6.06. The observed ^{13}C NMR data are consistent with the structure proposed by Ciavatta *et al.*[24] The chemical shift of the monomer (**1**) establishes the chemical shift region for the terminal ligands of the system. For the trimer (**2**), the low-frequency resonance

(38) Ferri, D.; Glaser, J.; Grenthe, I. *Inorg. Chim. Acta* **1988**, *148*, 133.
(39) Figgis, B. N.; Kidd, R. G.; Nyholm, R. S. *Proc. Royal Soc. A.* **1962**, *A269*, 469.
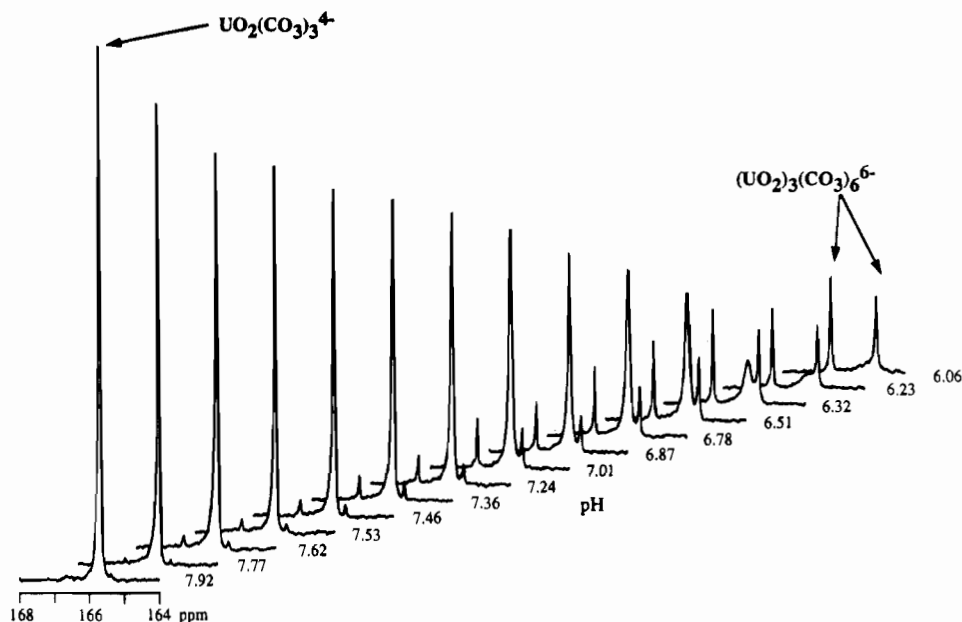
Figure 1. ^{13}C NMR spectra (62.9 MHz) of a 0.05 M uranyl carbonate solution at 2.5 m ionic strength as a function of pH recorded at 0 °C.

at δ 164.9 ppm can be assigned to the terminal carbonate ligand, and the high-frequency resonance at δ = 166.2 ppm to the bridging carbonate ligand. The integrated NMR resonances appear in a 1:1 bridge:terminal ratio. Warming the sample to ambient temperature results in a substantial increase in the linewidth of the high-field signal. This is further indication that the resonance at δ 164.9 is due to a terminal ligand since carbonate ligand exchange is expected to be more facile for a terminal ligand than a bridging ligand.[27]

Commensurate with the slowed exchange process at 0 °C, free bicarbonate and CO_2 are observed. Thus the exchange between free carbonate in solution and the terminal carbonate ligands in the uranyl carbonate complexes causes the line-broadening in the terminal carbonate resonance.

^{17}O NMR. Once the conditions that favored monomer and trimer formation were established by ^{13}C NMR, we sought to examine the solution species in further detail using ^{17}O NMR spectroscopy and to compare our results with the original ^{17}O data.[38] ^{17}O-enriched samples of the uranyl ions were prepared electrochemically, and carbonate solutions were prepared in a bomb reactor, as described in the Experimental Section. The ^{17}O NMR spectrum (33.9 MHz) for ^{17}O-enriched HCO_3^- at pH 8.3 shows a single, broad ($\Delta\nu_{1/2}$ = 400 Hz) resonance at δ 175 ppm, and a sample at pH 10.97 shows a resonance at 190.9 ppm ($\Delta\nu_{1/2}$ = 420 Hz). This compares favorably to the value of δ 192 ppm observed for the CO_3^{2-} ion in 0.1 M KOH solution.[39,40] Since the chemical shift is a weighted average of CO_3^{2-} and HCO_3^- chemical shifts, its position will be sensitive to pH. The broad linewidth of the HCO_3^- ion ($\Delta\nu_{1/2}$ = 400 Hz) is presumably the result of CO_3^{2-} + HCO_3^- chemical exchange. The observed chemical shift range of 175−190 ppm is in accord with the so-called "double-bond rule" as discussed by Klemperer.[41] The ^{17}O NMR spectrum of the UO_2^{2+} ion in 1 M $HClO_4$ revealed a chemical shift of δ 1121 ppm and can be compared to δ 1119 ppm reported by Fukutomi *et al.*[42,43]

An ^{17}O NMR spectrum of an ^{17}O-enriched sample of monomeric $U^*O_2(C^*O_3)_3^{4-}$ (**1**) recorded at pH 9.7 is shown in Figure 2. This spectrum revealed a uranyl oxygen in the expected chemical shift region at δ 1098 ppm and two other oxygen resonances in the carbonate oxygen region at δ 225 and 185 ppm (Figure 2). The uranyl oxygen resonance at δ 1098 is relatively sharp ($\Delta\nu_{1/2}$ = 6 Hz) as expected. Both resonances in the carbonate chemical shift region (Figure 2 insert) are very broad, indicative of chemical exchange. The resonance at δ 185 ppm is consistent with free CO_3^{2-} + HCO_3^- ions, and the broad resonance at δ 225 ppm is consistent with carbonate ligands in the coordination sphere of the uranyl ion.

The carbonate oxygen resonances seen at δ 185 and 225 at pH 9.7 (Figure 2 insert) undergo coalescence when the pH is lowered below 9. This is undoubtedly a result of an increase in the rate of carbonate ligand exchange with increasing hydrogen ion concentration. Examination of this system at a higher field strength (67.8 MHz) did not result in "freezing out" the chemical exchange of the carbonate ligands. Thus the carbonate oxygen resonances were never observed in this study below pH 9. In constrast, the uranyl oxygen resonances remain sharp as the pH is lowered, as these oxygen atoms do not exchange on the NMR time scale. The pH dependence of the uranyl oxygen region of the ^{17}O NMR spectra at 0 °C is extremely informative and is shown in the Figure 2 insert (33.9 MHz). At pH 7.87, there is a single uranyl-containing species with a resonance at δ 1098 ppm, assigned to monomeric $UO_2(CO_3)_3^{4-}$. As the pH is decreased, a second uranyl oxygen resonance appears at δ 1105 ppm. The resonance due to $UO_2(CO_3)_3^{4-}$ decreases while the new resonance assigned to the equivalent uranyl oxygen atoms in $(UO_2)_3(CO_3)_6^{6-}$ increases, until, at pH 6.0, the trimer, **2**, is the predominant uranyl-containing species in solution.

The ^{13}C and ^{17}O NMR data amassed thus far are consistent with the formation of trimeric $(UO_2)_3(CO_3)_6^{6-}$ as proposed by Åberg *et al.*[25] However, we admit that the ^{13}C and ^{17}O NMR resonances are equally consistent with formation of a dimer of formula $(UO_2)_2(CO_3)_4^{4-}$ (i.e. one bridge and one terminal ligand). For this reason, we examined this system using vibrational spectroscopy, extended X-ray absorption fine structure (EXAFS), and X-ray diffraction to obtain more definitive information regarding the structure in solution and the solid state.

(40) Boykin, D. W. *^{17}O NMR Spectroscopy in Organic Chemistry*; CRC Press: Boca Raton, FL, 1991.
(41) Klemperer, W. G. *Angew Chem., Int. Ed., Engl.* **1978**, *17*, 246.
(42) Jung, W.-S.; Ikeda, Y.; Tomiyasu, H.; Fukutomi, H. *Bull. Chem. Soc. Jpn.* **1984**, *57*, 2317.
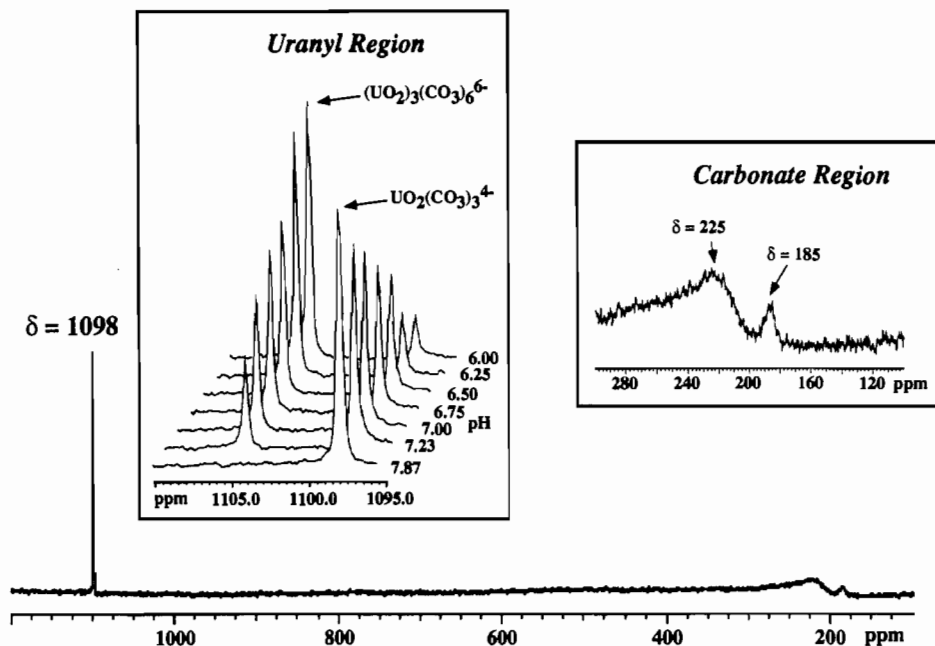(43) Jung, W.-S.; Tomiyasu, H.; Fukutomi, H. *Bull. Chem. Soc. Jpn.* **1985**, *58*, 938.

Figure 2. ^{17}O NMR spectrum (33.9 MHz) of fully ^{17}O-enriched $UO_2(CO_3)_3^{4-}$ at pH 9.7 and 0 °C. Inserts show (left) the expanded uranyl region of the ^{17}O NMR spectrum (33.9 MHz) of a 0.2 M $UO_2(CO_3)_3^{4-}$ solution as a function of pH at 0 °C and (right) the carbonate region (pH 9.7).

Solid Samples. Solution NMR studies and the thermodynamic data of Grenthe *et al.* revealed the conditions under which solutions of a single component could be prepared reproducibly. This allowed for the preparation of samples that contained nearly pure monomeric $UO_2(CO_3)_3^{4-}$ or trimeric $(UO_2)_3(CO_3)_6^{6-}$ anions. Countercations were added to the trimer solutions, followed by slow cooling to 5 °C under a CO_2 atmosphere, in multiple attempts to isolate crystalline samples suitable for X-ray diffraction studies. Either amorphous or microcrystalline precipitates or clear yellow solutions were obtained using Na^+, K^+, Me_4N^+, Et_4N^+, n-Pr_4N^+, and Ph_3MeN^+ countercations. We also examined the use of cryptands (Kryptofix 222, Kryptofix 211) or crown ethers (18-crown-6) in the presence of Na^+ or K^+ ions. None of these attempts provided crystalline samples. In contrast, the guanidinium cation $C(NH_2)_3^+$ yielded single crystals of compounds of empirical formula $[C(NH_2)_3]_4[UO_2(CO_3)_3]$ (**3**) and $[C(NH_2)_3]_2[UO_2(CO_3)_2]$ (**4**) on the basis of combustion elemental analysis. Crystals of $[C(NH_2)_3]_4[UO_2(CO_3)_3]$ (**3**) were suitable for single-crystal X-ray diffraction, while trimeric $[C(NH_2)_3]_6[UO_2(CO_3)_2]_3$ (**4**) formed small, thin plates that were unsuitable for single-crystal X-ray diffraction studies. However, the use of stoichiometric amounts of uranyl nitrate and guanidinium carbonate followed by the addition of 2 equiv of guanidinium nitrate produced crystals of formula $[C(NH_2)_3]_6[(UO_2)_3(CO_3)_6]\cdot6.5H_2O$ (**5**) which were suitable for single-crystal X-ray diffraction.

Vibrational Spectroscopy. Infrared spectra of crystalline samples of $[C(NH_2)_3]_4[UO_2(CO_3)_3]$, $[C(NH_2)_3]_6[(UO_2)_3(CO_3)_6]$, and $[C(NH_2)_3]_6[(UO_2)_3(CO_3)_6]\cdot6.5H_2O$ (Nujol mull and KBr pellet) showed vibrational bands characteristic of guanidinium ions, as well as characteristic group vibrational frequencies (ν_1, ν_2, ν_3, ν_4) for the carbonate ligand. It is well established that the carbonate ν_3 vibration is split into two components upon coordination to a metal ion.[44] This splitting is generally on the order of 50–60 cm^{-1} for monodentate and 160–190 cm^{-1} for bidentate coordination.[44] The splitting of the ν_3 mode by 181, 145, and 159 cm^{-1} (KBr) in crystalline samples of **3–5**, respectively, is consistent with bidentate or bridging carbonate

ligands. A resolved peak for the asymmetric O=U=O stretch was not observed in any guanidinium salt of the uranyl compounds. While the spectrum of **5** had an unresolved shoulder in the 915 cm^{-1} region, the uranyl peak was generally "masked" by the strong ν_2 carbonate out-of-plane deformation at 894, 895, and 892 cm^{-1} in **3–5**, respectively. However, a well-known relationship between Raman active (ν_1) and IR active (ν_3) O=U=O stretching modes allows for a calculation of the uranyl (ν_3) at 889 and 911 cm^{-1} from Raman data (vide infra) for **3** and **4**, respectively.[45]

Solution Raman spectra recorded on samples containing pure $UO_2(CO_3)_3^{4-}$ at pH 8.0 showed the symmetric ν_1(O=U=O) stretch at 812.5 cm^{-1}, while Raman spectra of a sample containing pure $(UO_2)_3(CO_3)_6^{6-}$ at pH 6.0 showed a significant shift in the ν_1(O=U=O) stretch to 831.6 cm^{-1}. The axial O=U=O force constant can be estimated to within 3% from the symmetric O=U=O stretching band ν_1 (Raman active) using the equation $k = 4.713 \times 10^{-6}[\nu_1^2 + (\nu_3^2/1.314)]$, where k is the force constant in mdyne/Å, ν is in cm^{-1}, and ν_3 is calculated from ν_1 as above.[46] For the monomeric species, $k = 6.088$ mdyne/Å, and for the trimeric species, $k = 6.094$ mdyne/Å. Therefore, the uranyl bond for the trimer is somewhat stronger than the monomer. The explanation of uranyl bond strength differences has been traditionally attributed to the strength of the equatorial bonding.[45] Specifically, ligand-to-metal σ- and π-bonding of the equatorial ligands pushes electron density toward the uranium metal center and increases electrostatic repulsion with the highly negative axial oxygen atoms to weaken the bonds. Therefore, weaker U=O$_{ax}$ bonds imply stronger equatorial bonding by carbonate ligands in the monomer than the trimer. Finally, application of a modified Badger's rule, as used by previous workers[46-49] through the equation $r = 1.08$ $k^{-1/3} + 1.17$, gives an axial U=O bond length of approximately 1.75 Å for both monomer and trimer. Note that this equation

(44) Jolivet, J. P.; Taravel, T. B.; Lorenzelli, V. *J. Mol. Struct.* **1980**, *60*, 93.

(45) McGlynn, S. P.; Smith, J. K.; Neely, W. C. *J. Chem. Phys.* **1961**, *35*, 105.
(46) Jones, L. H. *Spectrochim. Acta* **1958**, *10*, 395.
(47) Jones, L. H. *Spectrochim. Acta* **1959**, *11*, 409.
(48) Hoekstra, H. R. *Inorg. Chem.* **1963**, *2*, 492.
(49) Bullock, J. I. *J. Chem. Soc. A* **1969**, 781.

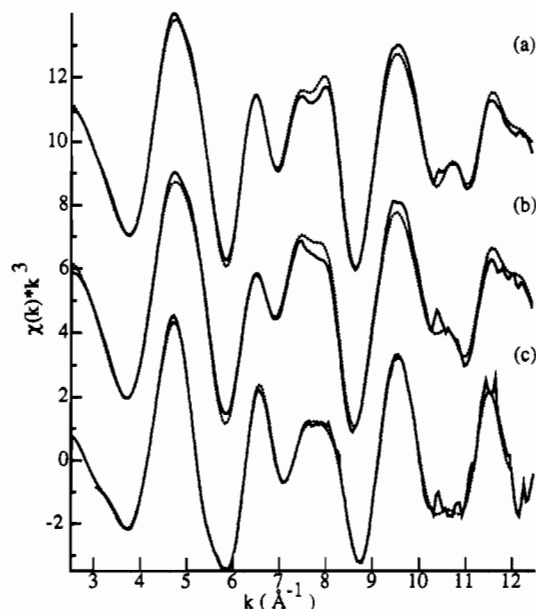**Figure 3.** Background-subtracted k^3-weighted EXAFS spectra of (a) solid $[C(NH_2)_3]_6[(UO_2)_3(CO_3)_6]$, (b) an aqueous solution of $(UO_2)_3$-$(CO_3)_6^{6-}$, and (c) solid $K_4[UO_2(CO_3)_3]$. The solid line is the experimental data, and the dotted line is the theoretical fit.

Figure 4. Fourier transforms without phase corrections of the k^3-weighted EXAFS of (a) solid $C(NH_2)_3]_6[(UO_2)_3(CO_3)_6]$, (b) an aqueous solution of $(UO_2)_3(CO_3)_6^{6-}$, and (c) solid $K_4[UO_2(CO_3)_3]$. The solid line is the experimental data, and the dotted line is the theoretical fit.

shows that vibrational frequencies are much more sensitive indicators for bond strengths than bond lengths.

EXAFS Studies. Single crystals of $[C(NH_2)_3]_6[(UO_2)_3$-$(CO_3)_6]$ formed as extremely thin plates that were unsuitable for single-crystal X-ray diffraction analysis. Therefore, we investigated the structure of $[C(NH_2)_3]_6[(UO_2)_3(CO_3)_6]$ by extended X-ray absorption fine structure (EXAFS) spectroscopy. In particular, a comparison of $[C(NH_2)_3]_6[(UO_2)_3(CO_3)_6]$ with a monomeric $M_4[UO_2(CO_3)_3]$ would confirm the presence of an oligomeric species if a U–U backscattering interaction was observed in the former. X-ray absorption measurements were performed at the uranium L_{III}-edge for three species, solid $[C(NH_2)_3]_6[(UO_2)_3(CO_3)_6]$, solid $K_4[UO_2(CO_3)_3]$, and a 0.2 M aqueous solution of ^{13}C-enriched $(UO_2)_3(CO_3)_6^{6-}$ at pH 5.7 under 1 atm of CO_2. ^{13}C NMR spectra of this solution were examined both before and after EXAFS analysis and indicated that $(UO_2)_3(CO_3)_6^{6-}$ was present in excess of 99% on the basis of NMR integration and that X-ray exposure did not result in any sample degradation. The theoretical EXAFS modeling code, FEFF6, of Rehr *et al.*[50,51] was employed to calculate the backscattering phases and amplitudes of the individual neighboring atoms, using the proposed structure **2** as a model. Background-subtracted k^3-weighted EXAFS spectra of crystalline $[C(NH_2)_3]_6[(UO_2)_3(CO_3)_6]$, an aqueous solution of $(UO_2)_3$-$(CO_3)_6^{6-}$, and crystalline $K_4[UO_2(CO_3)_3]$ are shown in Figure 3. Experimental data are shown as a solid line, and the theoretical fit is indicated as a dotted line. Fourier transforms (without phase corrections) of the k^3-weighted EXAFS of the three samples are shown in Figure 4. The solid line is the experimental data, and the dotted line is the theoretical fit.

Solid $[C(NH_2)_3]_6[(UO_2)_3(CO_3)_6]$ (4). The Fourier transform reveals five well-resolved peaks, labeled A–E in Figure 4a. The peaks occur at lower R values with respect to their true atomic positions due to the EXAFS phase shift ($\alpha \sim 0.2$–0.5 Å). Qualitative assignment of these peaks in terms of the model trimeric structure **2** is straightforward, with the exception of
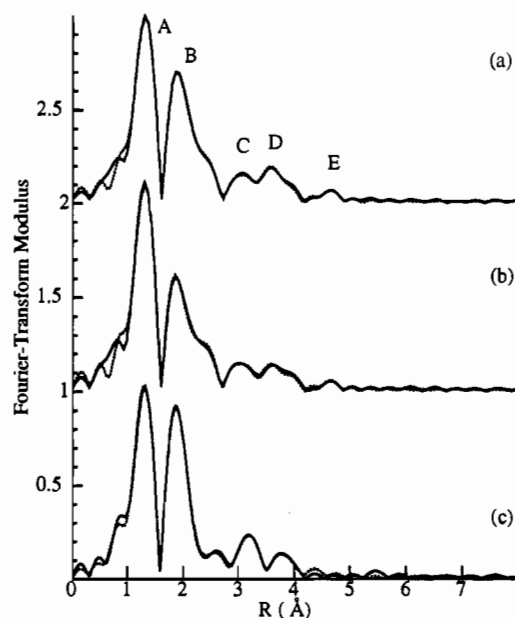
peak C. Peak A corresponds to the uranyl oxygens, while the asymmetric peak B arises from the six carbonate oxygens (bidentate ligation) in the equatorial plane together with the carbonate carbon atoms. The terminal oxygens of the carbonate groups give rise to peak D. The small peak at ca. 4.75 Å (E) may, at this level, be tentatively assigned to backscattering from the other uranium atoms of the trimeric unit.

Fitting of the experimental data on the basis of the preceding discussion is hampered by the existence of peak C, which at ca. 3.5 Å does not correspond to any single uranium–backscatterer distance in $UO_2(CO_3)_3^{4-}$ or in $(UO_2)_3(CO_3)_6^{6-}$. One possible source to consider for this interaction may be multiple scattering associated with the linear uranyl subunit. Multiple scattering is a well-established phenomenon in EXAFS spectroscopy[52–55] and contributes significantly when two or more atoms surrounding the photoabsorber are collinear. In this case peak C lies at an R value which is approximately twice that of peak A, suggesting multiple scattering along the uranyl vector as its origin. We have observed a similar peak in the Fourier transforms of the EXAFS for a variety of uranyl-containing compounds, including aqueous solutions of UO_2Cl_2.[56] Further support for this assertion is provided by FEFF6, which calculates a uranyl multiple scattering pathway with an effective R value twice the uranyl U–O distance. This path is calculated to have an amplitude ratio which is ~21% of the single scattering uranyl path. Additional theoretical modeling with FEFF6 reveals that multiple scattering effects are also significant for the terminal oxygens from the carbonates and the uranium neighbors in the trimer. In each case, a linear configuration exists (i.e., U–C–O and U–O–U), and multiple-scattering pathways along these units contribute significantly to the

(50) Mustre de Leon, J.; Rehr, J. J.; Zabinsky, S. I.; Albers, R. C. *Phys. Rev. B* **1991**, *44*, 4146.
(51) Rehr, J. J.; Mustre de Leon, J.; Zabinsky, S. I.; Albers, R. C. *J. Am. Chem. Soc.* **1991**, *113*, 5135.

(52) Teo, B. K. *J. Am. Chem. Soc.* **1981**, *103*, 3990.
(53) Teo, B. K. *EXAFS: Basic Principles and Data Analysis;* Springer-Verlag: Berlin, 1986.
(54) Garcia, J.; Delrio, M. S.; Buratini, E.; Benfatto, M. *Physica B* **1989**, *158*, 409.
(55) Vedrinskii, R. V.; Bugaev, L. A.; Levin, I. G. *Physica B* **1989**, *158*, 421.
(56) Bucher, J. J.; Edelstein, N. M.; Kaltsoyannis, N.; Lukens, W. W.; Shuh, D. K. Unpublished results.

Table 1. Structural Parameters from EXAFS Curve Fitting

shell	coord no.	r, Å	Debye−Waller factor, Å^2
Solid [C(NH$_2$)$_3$]$_6$[(UO$_2$)$_3$(CO$_3$)$_6$]			
U−O(uranyl)	2	1.79	0.0033
U−O(carbonate)	6	2.45	0.0080
U···C	3	2.90	0.0033
U···O(uranyl)^a		3.60^b	
U···O(carbonate)	3	4.16	0.0064
U···U	2	4.91	0.0081
Solution [(UO$_2$)$_3$(CO$_3$)$_6$]$^{6-}$			
U−O(uranyl)	2	1.79	0.0026
U−O(carbonate)	6	2.46	0.0075
U···C	3	2.90	0.0039
U···O(uranyl)^a		3.61^b	
U···O(carbonate)	3	4.17	0.0056
U···U	2	4.92	0.0087
Solid K$_4$[UO$_2$(CO$_3$)$_4$]			
U−O(uranyl)	2	1.79	0.0024
U−O(carbonate)	6	2.42	0.0059
U···C	3	2.89	0.0030
U···O(uranyl)^a		3.59^b	
U···K	6	3.84	0.0056
U···O(carbonate)	3	4.12	0.0046

^{a} Multiple scattering peak. ^{b} Effective r.

EXAFS Fourier transform peaks D and E, respectively. As a result, curve fits were performed using FEFF6 to model single scattering pathways for peaks A and B and multiple scattering pathways for peaks C−E.

Figure 4 shows the best fit (dotted line) obtained using this approach, and the fit parameters are given in Table 1. The fit quality is generally very good. The fitted EXAFS distances for [C(NH$_2$)$_3$]$_6$[(UO$_2$)$_3$(CO$_3$)$_6$] agree very closely with the X-ray crystallographic data for Na$_2$Ca[UO$_2$(CO$_3$)$_3$]·xH$_2$O ($x \approx 5.6$)[10] and K$_4$[UO$_2$(CO$_3$)$_3$].[57]

The most important result is the existence of peak E, whose EXAFS frequency and phase shift are characteristic of a U−U interaction at a distance of 4.91 Å. The EXAFS results are therefore consistent with an oligomeric structure for the uranium-containing component of [C(NH$_2$)$_3$]$_6$[(UO$_2$)$_3$(CO$_3$)$_6$]. However, due to the correlation between the coordination number and the Debye−Waller factor in fitting the EXAFS amplitude, the uncertainty in the U coordination number is such that EXAFS is unable to distinguish between a dimeric and a trimeric structure.

Aqueous [(UO$_2$)$_3$(CO$_3$)$_6$]$^{6-}$ (2). In order to obtain a more direct comparison with the NMR experiments, the EXAFS of the [(UO$_2$)$_3$(CO$_3$)$_6$]$^{6-}$-containing uranyl carbonate solution was investigated. Figure 3b shows the EXAFS spectrum, and Figure 4b shows its Fourier transform. The data are nearly identical to those of the solid compound (Figures 3a and 4a), with five well-resolved peaks in the transform, suggesting that the same species are present in both the solid and solution. In particular, the observation of peak E in the Fourier transform of the solution EXAFS lends further weight to the NMR evidence by supporting an oligomeric structure.

The experimental EXAFS was fitted using the same approach as for [C(NH$_2$)$_3$]$_6$[(UO$_2$)$_3$(CO$_3$)$_6$]. The results are given in Table 1. As before, the fit is very good. Once again we are unable to distinguish between a dimeric and a trimeric structure, but the EXAFS results are entirely consistent with the presence of an oligomeric species with a U−U distance of 4.92 Å.

Solid K$_4$[UO$_2$(CO$_3$)$_3$]. In order to verify the origin of the phase-shifted peak at 4.75 Å in the Fourier transforms of both

(57) Anderson, A.; Chieh, C.; Irish, D. E.; Tong, J. P. K. *Can. J. Chem.* **1980**, *58*, 1651.

Table 2. Summary of Crystallographic Data for [C(NH$_2$)$_3$]$_6$[(UO$_2$)$_3$(CO$_3$)$_6$]·6.5H$_2$O (**5**)

empirical formula	C$_{12}$H$_{49}$N$_{18}$O$_{30.5}$U$_3$
fw	1657.9
space group	$P\bar{1}$ (No. 2)
cell dimens	
a, Å	6.941(2)
b, Å	14.488(2)
c, Å	22.374(2)
α, deg	95.63(2)
β, deg	98.47(2)
γ, deg	101.88(2)
V, Å^3	2158.5
Z (molecules/cell)	2
D_{calc}, g cm^{-3}	2.551
μ, mm^{-1}	11.343
λ(Mo Kα), Å	0.710 73
temp, °C	−44
measd reflcns	11 695
unique intensities	9784
obsd reflcns	5482 ($F > 3\sigma(F)$)
$R(F)^a$	0.0555
$R_w(F)^b$	0.0607
goodness-of-fit	1.44

$^a R(F) = \Sigma||F_o| - |F_c||/\Sigma|F_o|.$ $^b R_w(F) = [\Sigma w(|F_o| - |F_c|)^2/ \Sigma w|F_o|^2]^{1/2}; w = 1/(\sigma^2(F)^2 + 0.0004F^2).$

[C(NH$_2$)$_3$]$_6$[(UO$_2$)$_3$(CO$_3$)$_6$] and the [(UO$_2$)$_3$(CO$_3$)$_6$]$^{6-}$-containing uranyl carbonate solution, we investigated the EXAFS for solid K$_4$[UO$_2$(CO$_3$)$_3$]. This monomeric compound should display EXAFS which is similar to that of the trimeric species but which has no U−U backscattering contribution. Figure 3c shows the EXAFS spectrum and Figure 4c shows its Fourier transform, both of which are quite similar to their counterparts in Figures 3 and 4. Closer inspection reveals some subtle differences in the Fourier transform of the monomer. That is, the uranyl multiple scattering resonance appears to be more intense and has shifted to higher R, and peak B appears to be sharper with a shoulder now on the high R side. Of key importance, however, is the absence of any peak beyond an R value of 4.0 Å, which provides further evidence to support the oligomeric nature of the uranium-containing species in both [C(NH$_2$)$_3$]$_6$[(UO$_2$)$_3$-(CO$_3$)$_6$] and the uranyl carbonate solution.

The experimental data were fit with the FEFF6 phases and amplitudes described previously for the trimeric compounds, however, with two important changes to the model. In this case, the U−U interaction was not included since it is apparently not observed in the raw EXAFS Fourier transform. In addition, examination of the crystal data for K$_4$[UO$_2$(CO$_3$)$_3$] reveals that six K atoms lie at ca. 3.81−3.85 Å from the central U. As a result, a shell of K atoms (using single scattering) was included in the fit. This latter contribution gives rise to a more complicated interference pattern in the monomer Fourier transform and helps to explain its different appearance with respect to the Fourier transforms of the trimeric compounds. The fitting results are given in Table 1. The agreement between the experimental and fitted Fourier transforms is very good. The results on K$_4$[UO$_2$(CO$_3$)$_3$] reinforce the conclusions drawn from the data on [C(NH$_2$)$_3$]$_6$[(UO$_2$)$_3$(CO$_3$)$_6$] and the uranyl carbonate solution and support the assertion that they contain oligomeric uranyl carbonate species.

Single Crystal X-ray Diffraction Studies. [CN$_3$H$_6$]$_6$-[(UO$_2$)$_3$(CO$_3$)$_6$]·6.5H$_2$O. X-ray quality crystals of **5** were grown by slow cooling of a concentrated aqueous solution of the uranyl carbonato trimer (**2**) containing excess guanidinium nitrate to 5 °C under a CO$_2$ atmosphere, and the structure was determined from diffraction data collected at −44 °C. Data collection and crystallographic parameters are summarized in Table 2. Fractional coordinates for the (UO$_2$)$_3$(CO$_3$)$_6$$^{6-}$ anionic unit are given

Table 3. Fractional Coordinates and Isotropic Thermal Parameters[a] for the Uranyl Anion in $[C(NH_2)_3]_6[(UO_2)_3(CO_3)_6] \cdot 6.5H_2O$ (**5**)

	$10^4 x$	$10^4 y$	$10^4 z$	$10^3 U$(eq), Å^2
U(1)	2944(1)	7179(1)	6592(1)	16(1)
U(2)	4520(1)	7183(1)	8830(1)	16(1)
U(3)	1937(1)	4123(1)	7453(1)	15(1)
O(101)	5513(19)	7216(8)	6564(6)	25(5)
O(102)	370(19)	7134(9)	6610(6)	26(5)
O(201)	7074(20)	7182(9)	8831(6)	32(5)
O(202)	1966(20)	7188(9)	8834(5)	27(5)
O(301)	4414(18)	3986(9)	7414(6)	26(5)
O(302)	−498(19)	4286(9)	7495(6)	30(5)
C(1)	1915(28)	5116(14)	6383(8)	22(7)
O(1)	2492(21)	5566(8)	6957(6)	29(5)
O(2)	1930(20)	5612(8)	5967(5)	24(5)
O(3)	1398(20)	4215(8)	6358(6)	25(5)
C(2)	3393(27)	5134(12)	8666(8)	17(6)
O(4)	3491(21)	5580(8)	8180(5)	25(5)
O(5)	4023(18)	5620(8)	9183(6)	22(5)
O(6)	2635(20)	4242(8)	8576(5)	25(5)
C(3)	4293(29)	8241(13)	7799(10)	28(7)
O(7)	3889(21)	7297(8)	7724(5)	25(5)
O(8)	4876(20)	8653(8)	8347(6)	27(5)
O(9)	4020(19)	8639(8)	7334(6)	27(5)
C(4)	2777(29)	8219(12)	5570(8)	22(6)
O(11)	2774(28)	8669(9)	5111(7)	56(7)
O(12)	3163(21)	8633(9)	6136(6)	34(5)
O(13)	2479(18)	7290(8)	5516(5)	23(4)
C(5)	5546(29)	8176(13)	10029(8)	25(7)
O(21)	6093(21)	8637(8)	10557(6)	29(5)
O(22)	5489(20)	8610(8)	9554(5)	25(5)
O(23)	5144(19)	7278(8)	9920(5)	22(4)
C(6)	725(29)	2082(14)	7339(8)	33(7)
O(31)	351(22)	1213(9)	7282(6)	33(5)
O(32)	1179(19)	2631(8)	7857(6)	24(5)
O(33)	616(19)	2572(8)	6855(5)	23(5)

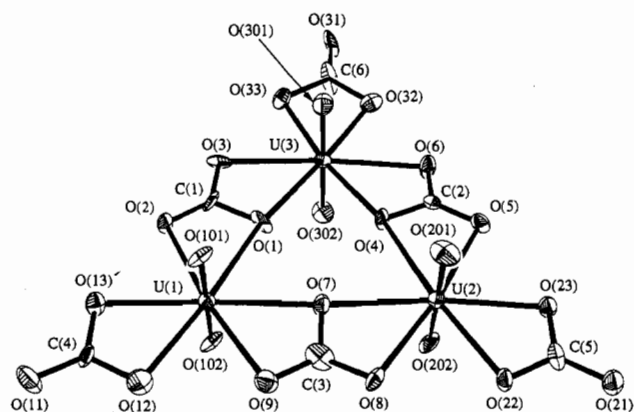[a] Equivalent isotropic U defined as one third of the trace of the orthogonalized U_{ij} tensor.

Table 4. Selected Bond Distances (Å) and Bond Angles (°) for the Uranyl Anion in $[C(NH_2)_3]_6[(UO_2)_3(CO_3)_6] \cdot 6.5H_2O$ (**5**)

U(1)−U(3)	4.965(1)	U(2)−O(5)	2.445(12)
U(1)−U(2)	4.959(1)	U(2)−O(7)	2.476(12)
U(2)−U(3)	4.978(1)	U(2)−O(8)	2.466(13)
U(1)−O(101)	1.783(14)	U(2)−O(22)	2.409(11)
U(1)−O(102)	1.781(14)	U(2)−O(23)	2.398(12)
U(1)−O(1)	2.525(12)	U(3)−O(301)	1.784(13)
U(1)−O(2)	2.456(10)	U(3)−O(302)	1.769(14)
U(1)−O(7)	2.502(12)	U(3)−O(1)	2.449(12)
U(1)−O(9)	2.467(11)	U(3)−O(3)	2.444(13)
U(1)−O(12)	2.416(13)	U(3)−O(4)	2.478(10)
U(1)−O(13)	2.406(12)	U(3)−O(6)	2.469(12)
U(2)−O(201)	1.773(14)	U(3)−O(32)	2.414(13)
U(2)−O(202)	1.775(14)	U(3)−O(33)	2.425(11)
U(2)−O(4)	2.523(10)		
O(101)−U(1)−O(102)	179.3(6)	U(1)−O(1)−U(3)	171.2(6)
O(201)−U(2)−O(202)	179.6(4)	U(2)−O(4)−U(3)	169.1(6)
O(301)−U(3)−O(302)	178.8(6)	U(1)−O(7)−U(2)	171.9(5)
O(101)−U(1)−O(1)	91.4(5)	U(1)−O(1)−C(1)	91.9(11)
O(102)−U(1)−O(1)	88.6(5)	U(3)−O(1)−C(1)	95.8(10)
O(101)−U(1)−O(2)	91.3(5)	U(1)−O(2)−C(1)	98.3(10)
O(102)−U(1)−O(2)	88.2(5)	U(3)−O(3)−C(1)	98.1(10)
O(1)−U(1)−O(2)	52.4(4)	U(1)−O(12)−C(4)	95.6(10)
O(1)−U(1)−O(7)	67.7(4)	U(1)−O(13)−C(4)	96.1(10)
O(2)−U(1)−O(9)	172.5(4)	O(1)−C(1)−O(2)	117.4(16)
O(7)−U(1)−O(9)	52.5(4)	O(1)−C(1)−O(3)	113.0(16)
O(1)−U(1)−O(12)	173.7(4)	O(2)−C(1)−O(3)	129.6(16)
O(9)−U(1)−O(12)	66.0(4)	O(11)−C(4)−O(12)	123.8(15)
O(2)−U(1)−O(13)	67.5(4)	O(11)−C(4)−O(13)	122.1(15)
O(7)−U(1)−O(13)	170.6(4)	O(12)−C(4)−O(13)	114.0(15)
O(12)−U(1)−O(13)	54.2(4)		

in Table 3, and selected bond lengths and angles for the $(UO_2)_3(CO_3)_6^{6-}$ unit are given in Table 4. An ORTEP drawing giving the atom-numbering scheme used in the tables is shown in Figure 5. The solid state molecular structure of $[C(NH_2)_3]_6$- $[(UO_2)_3(CO_3)_6] \cdot 6.5H_2O$ contains six guanidinium cations, 6.5 H_2O molecules, and a planar D_{3h} trimetallic $(UO_2)_3(CO_3)_6^{6-}$ anion, which are all involved in hydrogen bonding. The trimetallic anion contains three uranium atoms and all six carbonate ligands within a molecular plane. Three uranyl oxygen atoms lie above, and three lie below, the molecular plane. Uranyl O=U=O angles average 179.2(5)° with an average U=O distance of 1.78(1) Å. This distance can be compared with the 1.75 Å determined from vibrational spectroscopy and the 1.79 Å determined by EXAFS spectroscopy. This distance is comparable to the uranyl distances found in other uranyl-containing solids, and the distances of 1.80(2), 1.802(6), 1.79(1), 1.78(2), and 1.76(2) Å found in the solid state structures of $Na_2Ca[UO_2(CO_3)_3] \cdot 5.6H_2O$,[10] $K_4UO_2(CO_3)_3$,[57] $(NH_4)_4UO_2(CO_3)_3$,[29] $(CN_3H_6)_4[UO_2)(O_2)(CO_3)_2] \cdot 2H_2O$,[58] and $(CN_3H_6)_4[(UO_2)_2(C_4H_6N_2O_2)(CO_3)_3] \cdot H_2O$,[59] respectively. U−O distances to the carbonate ligands average 2.41(1) Å for terminal ligands, while bridging carbonates have somewhat longer distances of 2.48(1) Å (average). The terminal U−O carbonate distances are comparable to other terminal bidentate distances such as 2.44(1) and 2.430(5) Å seen in $Na_2CaUO_2(CO_3)_3 \cdot 5.6$ H_2O[10] and $K_4UO_2(CO_3)_3$,[57] respectively. To the best of our knowledge, the only other example of a bridging carbonate

ligand between uranyl centers in a discrete molecule is in the solid state structure of the dioximato complex $(CN_3H_6)_4[(UO_2)_2$- $(C_4H_6N_2O_2)(CO_3)_3] \cdot H_2O$.[59] The latter compound shows a distinct asymmetry in the bridging carbonate ligand in that the "internal" U−O distance is 2.38(1) while the four "external" U−O bonds average 2.53(2) Å.[59] We do not see any similar U−O asymmetries in our data. However, we do see statistically significant differences in the C−O bonds and O−C−O angles of the carbonate ligands. Terminal carbonate C−O bonds average 1.27(2) Å, and O−C−O angles average 114.0(16) and 123.0(16)°, with the smaller angle lying between oxygen atoms bound to the uranium centers. The bridging carbonate ligands show a significant asymmetry in C−O bond lengths. Internal C−O bond lengths [C(1)−O(1); C(2)−O(4); C(3)−O(7)] average 1.33(2) Å, while the six external C−O bonds average 1.26- (2) Å. Likewise, the six internal O−C−O angles average 116.5(15)°, while the three external angles average 127.0(15)°. For the bridging carbonate ligands, the U−O−U angles for the internal oxygen atoms [O(1), O(4), O(7)] are nearly linear and average 170.7(6)°. Particularly significant is the average

(58) Mikhailov, Y. N.; Lobanova, G. M.; Shchelokov, R. N. *Russ. J. Inorg. Chem.* **1981**, *26*, 386.
(59) Beirakhov, A. G.; Orlova, I. M.; Ashurov, Z. R.; Lobanova, G. M.; Mikhailov, Y. N.; Schelokov, R. N. *Russ. J. Inorg. Chem.* **1991**, *36*, 369.

Figure 5. ORTEP drawing of the $(UO_2)_3(CO_3)_6^{6-}$ anion giving the atom number scheme used in the tables.

Table 5. Comparison of X-ray and EXAFS Metrical Parameters

	X-ray		EXAFS	
	solid	soln	solid	soln
$UO_2(CO_3)_3^{4-}$				
U=O	1.80[a]		1.79[b]	
U—O(CO_3^{2-})	2.43		2.42	
U··C	2.88		2.89	
O=U=O	3.60		3.59	
U··O(CO_3^{2-})	4.12		4.12	
U··K	3.83		3.84	
$(UO_2)_3(CO_3)_6^{6-}$				
U=O	1.78[b]		1.79[b]	1.79[b]
U—O (CO_3^{2-})	2.46		2.45	2.46
U··C	2.88		2.90	2.90
O=U=O	3.54		3.60	3.61
U··O (CO_3^{2-})	4.14		4.16	4.17
U··U	4.97	4.95[c]	4.91	4.92

[a] Anderson, R.; Bombieri, B.; Forsellini, E. *J. Chem. Soc., Dalton Trans.* **1972**, 2059. [b] This work. [c] Åberg, M.; Ferri, D.; Glaser, J.; Grenthe, I. *Inorg. Chem.* **1983**, *22*, 3981.
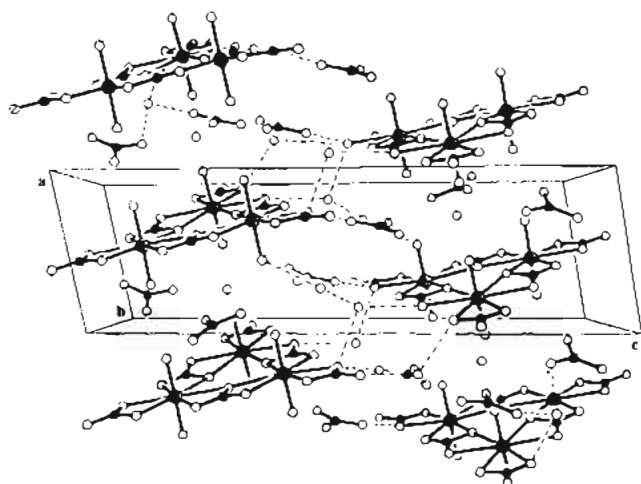

Figure 6. Ball-and-stick drawing looking down the crystallographic *b* axis and illustrating the packing of ions in $[C(NH_2)_3]_6[(UO_2)_3(CO_3)_6]\cdot5H_2O$.
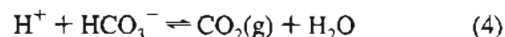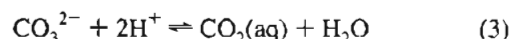
nonbonding U··U distance of 4.967(1) Å, which compares favorably to the 4.91 Å distance seen in the EXAFS analysis. A comparison of metrical parameters derived from EXAFS and X-ray diffraction data is given in Table 5. The agreement is excellent.

A ball-and-stick drawing illustrating the three dimensional packing and hydrogen bonding of $C(NH_2)_3^+$ and $(UO_2)_3(CO_3)_6^{6-}$ ions and H_2O molecules within the unit cell is shown in Figure 6. The planar guanidinium ions show average C—N distances of 1.32(2) Å. Both guanidinium cations and water molecules are involved in hydrogen-bonding interactions to the $(UO_2)_3$-$(CO_3)_6^{6-}$ anion. These interactions are quite strong as evidenced by short O··O contacts between water molecules and terminal or bridging carbonate oxygen atoms, which average 2.648(20) and 2.771(20) Å, respectively. In a similar fashion, short O··N contacts are observed between guanidinium nitrogen atoms and terminal or bridging carbonate oxygen atoms averaging 2.750(14) and 2.819(20) Å, respectively.

Analysis of Solution Thermodynamic Data. General Considerations. The EXAFS and X-ray diffraction studies have verified that trimeric $(UO_2)_3(CO_3)_6^{6-}$ is the predominant solution species at pH 6.0 under our experimental conditions of $[UO_2^{2+}] = 0.05$ M and $[CO_3^{2-} + HCO_3^-] = 0.15$ M. Therefore, the ^{13}C NMR integrations can be used to measure the monomer and trimer concentrations for a determination of the equilibrium constant for comparison with published ther-

modynamic data.[7] The published data have generally been measured under different conditions and need to be converted to a standard thermodynamic state to make meaningful comparisons. Second, an accurate determination of the hydrogen ion concentration was necessary.
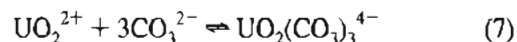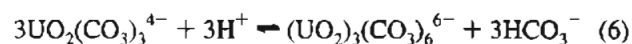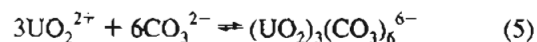
Hydrogen Ion Concentration; p[H]. To evaluate proton-dependent thermodynamic data, it is important to know $-\log [H^+]$ with high accuracy and precision.[60-62] Using the accepted equilibrium constants (Table 6) for the reactions shown in eqs 2–4,[7] one can calculate p[H][62] as a function of ionic strength

$$CO_3^{2-} + H^+ \rightleftharpoons HCO_3^- \qquad (2)$$

$$CO_3^{2-} + 2H^+ \rightleftharpoons CO_2(aq) + H_2O \qquad (3)$$

$$H^+ + HCO_3^- \rightleftharpoons CO_2(g) + H_2O \qquad (4)$$

using specific ion interaction theory and tabulated coefficients.[7] High ionic strength (2.5 and 3.0 m) buffer solutions were prepared by equilibrating solutions of $NaClO_4\cdot H_2O$ and $NaHCO_3$ with CO_2 gas mixtures of known compositions (Experimental Section). The pH electrode was calibrated using commercial pH buffer solutions, and then pH readings of our synthetic buffers were recorded after 48, 72, and 120 h and found to be stable. This calibration gives p[H] values, and at these ionic strengths, pH and p[H] values can differ by as much as 0.6 log units (Experimental Section).

Thermodynamic Equilibrium Constants. The distribution of species observed by multinuclear NMR can be compared with predictions based on data recorded under other conditions. In order to understand and model the total system, we considered hydrolysis, carbonate complexation, and carbonate/bicarbonate equilibria. Log equilibrium quotients at zero ionic strength for hydrolyzed uranyl species were taken from the recently published review of uranium data.[7] The solubility product for UO_2-$(OH)_2(s)$ was taken from Baes and Mesmer.[63] All the log equilibrium quotients used in our calculations are given in Table 6 (species other than those listed in the tables were not considered).

All of the log equilibrium quotients (log β's) were corrected for ionic strength using the specific ion interaction theory (SIT).[7] Osmotic coefficients were estimated to be the same as for $NaClO_4$ as given in Robinson and Stokes.[64] Quadratic equations for the osmostic coefficient as a function of concentration were fit to two concentration regions: 0.4 m $\leq I_m \leq$ 1.0 m and 1.0 m $\leq I_m \leq$ 4.0 m. The interaction coefficients used are from the uranium thermodynamic review.[7] Five determinations for the formation of the trimeric $(UO_2)_3(CO_3)_6^{6-}$ complex, log β_{36}, were reviewed by the Nuclear Energy Agency (NEA) for the reaction shown in eq 5. Those determinations were not

$$3UO_2^{2+} + 6CO_3^{2-} \rightleftharpoons (UO_2)_3(CO_3)_6^{6-} \qquad (5)$$

$$3UO_2(CO_3)_3^{4-} + 3H^+ \rightleftharpoons (UO_2)_3(CO_3)_6^{6-} + 3HCO_3^- \qquad (6)$$

$$UO_2^{2+} + 3CO_3^{2-} \rightleftharpoons UO_2(CO_3)_3^{4-} \qquad (7)$$

consistent, and the NEA review selected the unweighted average of these values to be log $\beta^0_{36} = 54.0 \pm 1.0$.[7] The observation

(60) Westcott, C. C. *pH Measurements*; Academic Press: New York, 1978.
(61) Linder, P. W.; Torrington, R. G.; Williams, D. R. *Analysis Using Glass Electrodes*; Open University Press: Milton Keynes, U.K., 1984.
(62) Martell, A. E.; Motekaitis, R. J. *Determination and Use of Stability Constants*; VCH Publishers: New York, 1988.
(63) Baes, C. F.; Mesmer, R. E. *The Hydrolysis of Cations*; J. Wiley and Sons: New York, 1976.

Table 6. Thermodynamic Constants for the Uranyl Carbonate System Used in This Study[a]

					I_m		
					0	2.5	3.0
Ligand Data							
$CO_3^{2-} + H^+$		$\rightleftharpoons$	HCO_3^-	$\log K =$	10.33	9.68	9.71
$CO_3^{2-} + 2H^+$		$\rightleftharpoons$	$CO_2(aq) + H_2O$	$\log K =$	16.68	15.82	15.90
$HCO_3^- + H^+$		$\rightleftharpoons$	$CO_2(g) + H_2O$	$\log K =$	7.82	7.65	7.70
Metal Complex Data							
$UO_2^{2+} + CO_3^{2-}$		$\rightleftharpoons$	$UO_2(CO_3)(aq)$	$\log \beta_{11} =$	9.63	8.87	9.05
$UO_2^{2+} + 2CO_3^{2-}$		$\rightleftharpoons$	$UO_2(CO_3)_2^{2-}$	$\log \beta_{12} =$	16.94	15.78	15.88
$UO_2^{2+} + 3CO_3^{2-}$		$\rightleftharpoons$	$UO_2(CO_3)_3^{4-}$	$\log \beta_{13} =$	21.63	22.18	22.29
$3UO_2^{2+} + 6CO_3^{2-}$		$\rightleftharpoons$	$(UO_2)_3(CO_3)_6^{6-}$	$\log \beta_{36} =$	54.00	55.32	55.59
Metal Hydrolysis Data							
$UO_2^{2+} + H_2O$		$\rightleftharpoons$	$UO_2(OH) + H^+$	$\log \beta_{1-1} =$	−5.20	−4.71	−4.54
$2UO_2^{2+} + H_2O$		$\rightleftharpoons$	$(UO_2)_2(OH)^{3+}$	$\log \beta_{2-1} =$	−2.70	−2.26	−2.25
$UO_2^{2+} + 2H_2O$		$\rightleftharpoons$	$UO_2(OH)_2 + 2H^+$	$\log \beta_{1-2} =$	−10.30	−10.40	−10.34
$2UO_2^{2+} + 2H_2O$		$\rightleftharpoons$	$(UO_2)_2(OH)_2^{2+} + 2H^+$	$\log \beta_{2-2} =$	−5.62	−6.05	−6.05
$3UO_2^{2+} + 4H_2O$		$\rightleftharpoons$	$(UO_2)_3(OH)_4^{2+} + 4H^+$	$\log \beta_{3-4} =$	−11.90	−13.25	−13.36
$3UO_2^{2+} + 7H_2O$		$\rightleftharpoons$	$(UO_2)_3(OH)_7^- + 7H^+$	$\log \beta_{3-7} =$	−31.00	−32.46	−32.60
$3UO_2^{2+} + 5H_2O$		$\rightleftharpoons$	$(UO_2)_3(OH)_5^+ + 5H^+$	$\log \beta_{3-5} =$	−15.55	−16.74	−16.74
$4UO_2^{2+} + 7H_2O$		$\rightleftharpoons$	$(UO_2)_4(OH)_7^+ + 7H^+$	$\log \beta_{4-7} =$	−21.90	−23.17	−23.10

[a] Values at $I_m = 0$ taken from ref 7 and corrected using SIT.

of this species by multinuclear NMR provides an opportunity to refine this value. In our NMR experiments, the experimental observables were those indicated in eq 6, and hence we cannot determine $\log \beta_{36}$ directly. Quantitative ^{13}C NMR experiments were performed for a 0.05 M uranyl sample with an ionic strength of 2.5 m in order to examine the equilibrium constant for the reaction shown in eq 6. Accurate NMR integrations were possible in the range of p[H] between 7.3 and 7.7. At p[H] lower than 7.3, CO_2 had to be placed over the solution to stabilize the p[H]; hence, the carbonate concentration could not be known accurately. The four measurements obtained in this range give $\log K = 18.1(\pm 0.5)$ at 2.5 m ionic strength and 25 °C for eq 6. We used specific ion interaction theory and the interaction coefficients recommended by the NEA to calculate the equilibrium constants for eqs 2−4 and 7 at 2.5 m ionic strength. These values are indicated in Table 6. These values were then used to calculate $\log \beta_{36} = 55.6(\pm 0.5)$ for eq 5 at 2.5 m and 25 °C via ^{13}C NMR data. This value can be compared with the calculated value from the NEA review at 2.5 m (Table 6) of $\log \beta_{36} = 55.32(\pm 1.0)$. The agreement is excellent.

Concluding Remarks

The ^{13}C and ^{17}O NMR, IR, and Raman experiments are consistent with the formation of $(UO_2)_3(CO_3)_6^{6-}$, as originally proposed by Ciavatta *et al.*[17] EXAFS data from solid $[C(NH_2)_3]_6$-$[(UO_2)_3(CO_3)_6]$ and a solution of $(UO_2)_3(CO_3)_6^{6-}$ suggest that the same uranium species is present in both the solid and solution states. Fourier transforms of the EXAFS spectra of both solid and solution samples revealed five well-resolved peaks corresponding to U=O = 1.79, U−O(carbonate) = 2.45, U--C = 2.90, U--O(carbonate) = 4.16, and U--U = 4.91 Å for the solid and similar distances for the solution sample. The peak at 4.75 Å in both Fourier transforms (uncorrected for phase shift) corresponds to the U--U interaction at 4.91 Å, a conclusion which is supported by the absence of the peak in the Fourier transform of crystalline monomeric $K_4[UO_2(CO_3)_3]$. Multiple scattering along the uranyl vector is believed to play a significant role in the EXAFS of all three systems. The EXAFS data are therefore consistent with the trimeric uranyl carbonate species indicated by NMR spectroscopy. The solid

state molecular structure of $[C(NH_2)_3]_6[(UO_2)_3(CO_3)_6]\cdot 6.5H_2O$ confirms a planar D_{3h} trimetallic $(UO_2)_3(CO_3)_6^{6-}$ anion as originally proposed by Åberg *et al.*[25] Particularly significant is the average nonbonding U--U distance of 4.97 Å, which compares favorably to the 4.91 Å distance seen in the EXAFS spectrum, and the 4.95 Å distance, seen by solution X-ray diffraction.[25] The NMR data allows for the determination of $\log \beta_{36} = 55.6(\pm 0.5)$ at 2.5 m and 25 °C, which is in excellent agreement with the value recommended by the NEA.[7]

Uranium(VI) is by far the most well-studied actinide system available, and the reviewers of the uranium(VI) literature[7] appear to have done an outstanding job of critically analyzing this data and suggesting a suitable set of thermodynamic constants for hydrolysis and carbonate complexation of uranium(VI). This NMR study validates a subset of these thermodynamic constants. Future multinuclear NMR studies of the important transuranic systems will provide insight for choosing the best model to fit new and existing thermodynamic data. This multiple method approach should provide the most accurate estimate of thermodynamic constants for use in geochemical, site assessment, and performance assessment modeling. Further studies of An(VI) and An(V) (An = Np, Pu, Am) carbonate complexation by multinuclear NMR, EXAFS, and X-ray diffraction are in progress.

Experimental Section

General Considerations. All manipulations were carried out inside fume hoods or negative pressure gloveboxes designed for containment of radioactive materials. Standard radiochemical procedures were used throughout. Ultrapure $HClO_4$, "Supra-pure" NaOH, and sodium perchlorate monohydrate (Fluka) were used without purification. Sodium carbonate, sodium bicarbonate, and guanidine carbonate (Aldrich) were used without further purification. Guanidinium nitrate was prepared from guanidine carbonate and nitric acid. D_2O (99.9% D) and ^{13}C-enriched Na_2CO_3 (99.9% [13]C) were purchased from Cambridge Isotopes. Deuterium oxide was degassed by bubbling with argon for 1 h, and the Na_2[13]CO_3 was used as received. [17]O-enriched H_2O (20% [17]O) was obtained from Los Alamos National Laboratory stock and used without further purification. $UO_2(ClO_4)_2(H_2O)_6$ was recrystallized 3 times from perchloric acid. pH was measured using a Corning model 130 pH meter and an Orion (Ross, Model 8103) combination electrode. Carbon dioxide gas was humidified by bubbling through a 3.0 M KCl solution prior to passing over samples in order to maintain a constant vapor pressure and minimize evaporation of sample solutions.

(64) Robinson, R. A.; Stokes, R. H. *Electrolyte Solutions*; Butterworths Scientific Publications: London, 1955; p 28.

Solution UV—visible—near-IR spectra were recorded using a Perkin-Elmer Lambda 9 Spectrophotometer and matched 1.0 or 0.1 cm quartz cells. Electrochemical syntheses of ^{17}O-labeled actinide solutions were performed using an EG&G PARR Model 173 potentiostat/coulometer. Electrochemical cells used for bulk electrolysis had separate compartments for reference and counter electrodes and are described in detail elsewhere.[65] A Pt screen working electrode was separated from a Pt wire counter electrode by a Vicor frit, and a saturated calomel electrode (SCE) was used as a reference electrode. Elemental analyses were performed on a Perkin-Elmer 2400 CHN analyzer. Infrared spectra were recorded as KBr pellets or as Nujol mulls between KBr plates on a Digilab FTS-40 spectrometer. Elemental analysis samples were prepared and sealed in tin capsules in the glovebox prior to combustion.

All NMR sample solutions were loaded into Wilmad 5 mm o.d. 507-PP Pyrex glass NMR tubes which were flame-sealed with a small hand torch. Variable-temperature FT ^{13}C and ^{17}O NMR spectra were recorded on a Bruker AF 250 spectrometer fitted with a 5 mm broadband probe operating at 62.9 (^{13}C) or 33.9 (^{17}O) MHz, on a Varian Unity 300 spectrometer with a 5 mm broadband probe operating at 75.4 (^{13}C) or 40.7 (^{17}O) MHz, or on a Bruker AMX500 spectrometer with a 5 mm broadband probe operating at 67.8 (^{17}O) MHz with ^2H field-frequency lock. The ^{13}C $\pi/2$ pulse length was measured to be 5.25 (62.9 MHz) and 17.0 μs (75.4 MHz) using the free carbonate resonance. The ^{17}O $\pi/2$ pulse length was measured to be 11.8 (33.9 MHz) and 13.8 μs (67.8 MHz) using the free water resonance. The temperature was controlled with Bruker or Varian variable-temperature controllers and was stable to within ± 1 K. The temperature was determined by measurement of the ^1H NMR of ethylene glycol (295—350 K) or methanol (270—295 K) at the same temperature and gas flow rate. All ^{13}C NMR chemical shifts are reported in ppm relative to the carbonyl carbon of external acetone-d_6 set at $\delta = 206.0$. All ^{17}O NMR chemical shifts are reported in ppm relative to external H_2O set at $\delta = 0$.

Preparation of Bicarbonate p[H] Buffers. Buffer solutions were prepared by equilibrating solutions of $NaClO_4$ and $NaHCO_3$ with CO_2 gas mixtures of known compositions. All buffers were transferred to gas scrubbers and saturated with the appropriate gas mixtures. An Orion Ross combination electrode was calibrated with commercial buffers at pH = 7 and pH = 10 on an Orion ion analyzer, and then pH readings of our bicarbonate pH buffers were recorded after 48, 72, and 120 h and found to be stable. Density readings for each synthetic buffer were obtained by weighting 10 mL of each solution. A barometric pressure of 570 mmHg (7300 ft above sea level) was used.

Ionic Strength 3.0 m. p[H] was plotted against pH, and linear regression gave the following pH correction for experiments at an ionic strength $I_m = 3.0$ m. p[H] = 1.00828(pH) + 0.520468, $R^2 = 0.9996$. Buffer no. 1, p[H] = 8.70. A 27.34 mL volume of 8.93 M $NaClO_4$ solution (244.15 mmol) and 1.6803 g (20.00 mmol) of $NaHCO_3$ were combined and dissolved with 100 mL of distilled water in a volumetric flask to give a solution of composition 2.4415 M $NaClO_4$, 0.2 M $NaHCO_3$, $\varrho = 1.2013$ g/mL, and $I = 3.00$ m. This solution was bubbled with 3% (f-CO_2 = 0.03) CO_2—Ar to establish equilibrium. Buffer no. 2, p[H] = 7.76. A 27.34 mL volume of 8.93 M $NaClO_4$ solution (244.15 mmol) and 1.6818 g (20.02 mmol) of $NaHCO_3$ were combined and dissolved with 100 mL of distilled water in a volumetric flask to give a solution of composition 2.4415 M $NaClO_4$, 0.2002 M $NaHCO_3$, $\varrho = 1.2039$ g/mL, and $I = 2.98$ m. This solution was bubbled with 30.2% (f-CO_2 = 0.302) CO_2—Ar to establish equilibrium. Buffer no. 3, p[H] = 6.98. A 36.5121 g (259.95 mmol) amount of $NaClO_4 \cdot H_2O$ and 0.8419 g (10.02 mmol) of $NaHCO_3$ were combined and dissolved with 100 mL of distilled water in a volumetric flask to give a solution of composition 2.5998 M $NaClO_4$, 0.1002 M $NaHCO_3$, $\varrho = 1.1964$ g/mL, and $I = 3.10$ m. This solution was bubbled with 100% (f-CO_2 = 1.0) CO_2 to establish equilibrium. Buffer no. 4, p[H] = 5.99. A 36.8247 g (262.27 mmol) amount of $NaClO_4 \cdot H_2O$ and 0.0869 g (1.03 mmol) of $NaHCO_3$ were dissolved with 100 mL of distilled water in a volumetric flask to give a solution of composition 2.6221 M $NaClO_4$, 0.0103 M $NaHCO_3$, $\varrho = 1.1886$ g/mL, and $I = 3.04$ m. This solution was bubbled with 100% (f-CO_2 = 1.0) CO_2 to establish equilibrium.

Ionic strength 2.5 m. p[H] was plotted against pH, and linear regression gave the following pH correction for experiments at an ionic strength $I_m = 2.5$ mol/kg. p[H] = 1.00828(pH) + 0.520468, $R^2 = 0.9999$. Buffer no. 1, p[H] = 8.65. A 28.6538 g (204 mmol) amount of $NaClO_4 \cdot H_2O$ and 1.6800 g (20 mmol) of $NaHCO_3$ were dissolved with 100 mL of distilled water in a volumetric flask to give a solution of composition 2.0403 M $NaClO_4$, 0.2 M $NaHCO_3$, $\varrho = 1.16$ g/mL, and $I = 2.52$ m. This solution was bubbled with 3% (f-CO_2 = 0.03) CO_2—Ar to establish equilibrium. Buffer no. 2, p[H] = 7.71. A 28.795 g (205 mmol) amount of $NaClO_4 \cdot H_2O$ and 1.6800 g (20 mmol) of $NaHCO_3$ were dissolved with 100 mL of distilled water in a volumetric flask to give a solution of composition 2.0501 M $NaClO_4$, 0.2 M $NaHCO_3$, $\varrho = 1.16$ g/mL, and $I = 2.52$ m. This solution was bubbled with 30.2% (f-CO_2 = 0.302) CO_2—Ar to establish equilibrium. Buffer no. 3, p[H] = 6.89. A 30.1993 g (215 mmol) amount of $NaClO_4 \cdot H_2O$ and 0.8412 g (10 mmol) of $NaHCO_3$ were dissolved with 100 mL of distilled water in a volumetric flask to give a solution of composition 2.150 M $NaClO_4$, 0.1001 M $NaHCO_3$, $\varrho = 1.17$ g/mL, and $I = 2.51$ m. This solution was bubbled with 100% (f-CO_2 = 1.0) CO_2—Ar to establish equilibrium. Buffer no. 4, p[H] = 5.89. A 31.3225 g (223 mmol) amount of $NaClO_4 \cdot H_2O$ and 0.084 g (1 mmol) of $NaHCO_3$ were dissolved with 100 mL of distilled water in a volumetric flask to give a solution of composition 2.230 M $NaClO_4$, 0.010 M $NaHCO_3$, $\varrho = 1.17$ g/mL, and $I = 2.50$ m. This solution was bubbled with 100% (f-CO_2 = 1.0) CO_2—Ar to establish equilibrium.

Solution Preparations. ^{17}O-Enriched Solutions. Crystalline $UO_2(ClO_4)_2(H_2O)_6$ (0.577 g, 1.0 mmol) was dissolved in 2.5 mL of 20.4% $H_2^{17}O$ and 0.250 mL of 10.7 M ultrapure $HClO_4$ to prepare a 20% ^{17}O-enriched solution of 0.4 M UO_2^{2+} ion in 1 M $HClO_4$. This uranyl solution was electrolytically reduced to aquo U^{4+} using a conventional 3-electrode system at a potential of -0.22 V (vs SCE). The uranium solution was electrochemically re-oxidized to the UO_2^{2+} ion at about 1.10 V (vs SCE). This resulted in a UO_2^{2+} solution that was 10% enriched in ^{17}O. The oxidation states were confirmed using UV—vis-near-IR spectroscopy to identify the U(IV) peak at 648 nm ($\epsilon = 59$ M^{-1} cm^{-1})[66] and the U(VI) peak at 414 nm ($\epsilon = 7.6$ M^{-1} cm^{-1})[67] at each stage of the electrolysis. The $U^{17}O_2^{2+}$ was then precipitated as the hydroxide between $4.5 \leq$ pH ≤ 7. The precipitate was isolated by centrifugation and then washed 3 times with distilled, deionized H_2O. A solution of ^{17}O-labeled carbonate was made by combining 2.32 mL of 43% $H_2^{17}O$, 2.4 mL of D_2O, and 0.28 mL of 10.7 M supra-pure (carbonate-free) NaOH to make a 0.6 M NaOH solution. This solution was placed in a PARR pressure vessel and charged with 5 atm of CO_2 with stirring. The solution was allowed to equilibrate for 48 h, to produce 5 mL of 0.6 M ^{17}O-enriched $NaHCO_3$. The ^{17}O-enriched uranyl hydroxide precipitate was dissolved in 4.25 mL of the freshly-prepared ^{17}O-enriched $NaHCO_3$. The resulting slurry was mixed on a vortex mixer for several minutes and then placed in an ultrasonic bath for 10 min until all the solid had dissolved, and a clear yellow solution resulted. $NaClO_4 \cdot H_2O$ (0.598 g, 7.1 mmol) was added to adjust the ionic strength to 3.3 mol/kg. A 1 M $HClO_4$ solution and solid Na_2CO_3 were used to adjust the pH and obtain samples in the pH range from $6.0 \leq$ pH ≤ 9.7. Samples were sealed in 5 mm NMR tubes, and solutions near a pH of 6 were stabilized by using CO_2-flushed NMR tubes. Samples flushed with CO_2 were not used in thermodynamic calculations.

Solution Preparations. ^{13}C-Enriched Solutions. Crystalline $UO_2(ClO_4)_2(H_2O)_6$ (1.739 g, 3.0 mmol) was dissolved in 2.0 mL of D_2O. $Na_2^{13}CO_3$ (0.954 g, 8.9 mmol) and $NaClO_4 \cdot H_2O$ (2.104 g, 25 mmol) were dissolved in 13 mL of D_2O in a 50 mL Oak Ridge centrifuge tube. The uranium solution was slowly added to this carbonate solution with stirring to make a solution which was 0.2 M in uranium, 0.6 M in sodium carbonate, and 1.0 M in sodium perchlorate. A 1 M $HClO_4$ solution was used to adjust the pH of the solution to prepare five samples with pH values ranging from pH 9.04 to 5.97. Samples were sealed in standard 5 mm NMR tubes; those at lower pH were sealed in tubes flushed with CO_2 to maintain the pH. Another sample at $I_m = 2.5$ m was prepared similarly to make a solution which was 0.05 M in uranium, 0.15 M in sodium carbonate, and 1.8 M in $NaClO_4$. A 1 M

(65) Hobart, D. E.; Samhoun, K.; Peterson, J. R. *Radiochim. Acta* **1982**, *31*, 139.

(66) Kraus, K. A.; Nelson, F. *J. Am. Chem. Soc.* **1950**, *72*, 3901.
(67) Sjoblom, R.; Hindman, J. C. *J. Am. Chem. Soc.* **1951**, *73*, 1744.

HClO$_4$ solution was used to adjust the pH of the solution to prepare 17 samples with pH values ranging from pH 9.0 to 5.7. Samples were sealed in standard 5 mm NMR tubes; those at lower pH were sealed in tubes flushed with CO$_2$ to maintain the pH.

Synthesis of [C(NH$_2$)$_3$]$_4$[UO$_2$(CO$_3$)$_3$] (3). To a solution of 0.504 g (1.0 mmol) of UO$_2$(NO$_3$)$_2$·6H$_2$O in 0.5 mL of distilled water, a solution of 0.541 g (3.0 mmol) of guanidine carbonate in 9.5 mL of distilled water was added dropwise with stirring. The resulting 10 mL of solution was 0.1 M in uranium and 0.3 M in carbonate and had a pH of 9.53. The solution was sealed in an argon-purged 20 mL glass scintillation vial, wrapped in Parafilm, and stored at 0 °C. After 24 h, large cubic crystals of a bright-yellow crystalline solid resulted. IR (KBr plates, Nujol, cm^{-1}): 3475 (vs, br), 1687 (s), 1526 (s), 1343 (s), 1143 (m), 1054 (m), 892(s), 866 (m), 811 (w), 687 (m), 530 (m). IR (KBr pellet, cm^{-1}): 1692 (s) 1521 (s, br), 1340 (s, br), 1139 (m), 1046 (m), 894 (s), 860 (m), 725 (m), 684 (w). Anal. Calcd for UO$_{17}$N$_{12}$C$_7$H$_{24}$: C, 12.19; H, 3.50; N, 24.35. Found: C, 12.95; H, 3.22; N, 23.74.

Synthesis of [C(NH$_2$)$_3$]$_6$[(UO$_2$)$_3$(CO$_3$)$_6$] (4). To a solution of 0.504 g (1.0 mmol) of UO$_2$(NO$_3$)$_2$·6H$_2$O in 0.5 mL of distilled water was added dropwise a solution of 0.541 g (3.0 mmol) of guanidine carbonate in 9.5 mL of distilled water with stirring. The resulting 10 mL of solution was 0.1 M in uranium and 0.3 M in carbonate. The pH of the uranyl carbonate solution was slowly lowered using 1 M HCl, and a stream of CO$_2$ was passed over the solution to reach a final pH of 6.12. The solution was then sealed in a CO$_2$-purged 20 mL glass scintillation vial, wrapped in Parafilm, and stored at 0 °C. After 24 h, thin needlelike plates of a bright-yellow crystalline solid resulted. IR (Nujol, KBr plates, cm^{-1}): 3352 (vs, br), 1672 (s), 1519 (s), 1464 (s), 1378 (s), 1339 (s), 1141 (m), 1047 (m), 886(s), 731 (s), 535 (m). IR (KBr pellet, cm^{-1}): 1668 (s), 1574 (m), 1528 (s), 1383 (s), 1333 (m), 1056 (w), 895(s), 835 (m), 728 (m), 713 (w). Anal. Calcd for U$_3$O$_{24}$N$_{18}$C$_{12}$H$_{36}$: C, 9.42; H, 2.37; N, 16.47. Found: C, 10.21; H, 2.61; N, 19.00.

Synthesis of [C(NH$_2$)$_3$]$_6$[(UO$_2$)$_3$(CO$_3$)$_6$]·6.5H$_2$O (5). A solution of 0.502 g (1.0 mmol) of UO$_2$(NO$_3$)$_2$·6H$_2$O in 5 mL of distilled water was added to 5 mL of aqueous guanidine carbonate (0.540 g, 3.00 mmol) to yield a clear yellow solution. The pH of the resulting solution was adjusted to pH 7 using 0.1 M HClO$_4$. Guanidine nitrate (0.732 g, 6.00 mmol) was added, and the solution was purged with CO$_2$. A fine white precipitate formed rapidly. The solution was stirred vigorously for several days, after which the solution was centrifuged and the supernatant was removed via pipet. The pH of the supernatant solution was measured to be 7.1. The solution was then blanketed with an atmosphere of CO$_2$ and cooled to 4 °C. After 2 days, yellow cube-shaped crystals (believed to be [C{NH$_2$)$_3$]$_4$[UO$_2$(CO$_3$)$_4$]·nH$_2$O) had formed. Slowly, yellow needle-shaped crystals of **5** began to form. After 30 days, several large needles had formed. IR (KBr, cm^{-1}): 3405 (vs), 3377 (sh), 3198 (s), 1665 (s), 1578 (s, sh), 1530 (s), 1371 (s), 1149 (w), 1047 (m), 914 (s), 892 (s), 843 (m), 728 (m).

Raman Measurements. Raman vibrational spectra were obtained by excitation from an Ar$^+$ laser (Spectra Physics, Model 2025) using the 363.8 nm line. The laser power at the sample was ~10 mW. The scattered light was dispersed and analyzed on a SPEX Model 1403 scanning double monochromator equipped with an 1800 groove/mm grating and a single-photon-counting detector. The spectral slit width was maintained at 4 cm^{-1} resolution. Scan parameters were 1 cm^{-1} increments between points, integration for 2 s at each point, and at least 60 scans averaged for the final spectrum. Spectra were recorded on ^{13}C-enriched samples in sealed 5 mm NMR tubes.

EXAFS Studies. The EXAFS measurements were performed at the storage ring of the Stanford Synchrotron Radiation Laboratory (SSRL) on wiggler beamlines 4-3 and 4-1. Uranium L$_{III}$ edge (~17.17 keV) spectra were recorded with Si(220) monochromator crystals (detuned 50% to reduce higher order harmonic content). All of the data were obtained from transmission experiments, in which argon gas ionization chamber detectors were employed. All spectra were collected simultaneously with uranium reference materials to establish the respective chemical shifts and to ensure photon energy calibrations. A total of 8−10 scans of approximately 1 h duration were required to obtain good data on [C(NH$_2$)$_3$]$_6$[(UO$_2$)$_3$(CO$_3$)$_6$] and the [(UO$_2$)$_3$(CO$_3$)$_6$]$^{6-}$-containing uranyl carbonate solution. Data analysis, including EXAFS curve fitting, was performed with the EXAFSPAK program suite, written by Graham N. George at SSRL. NMR studies of a duplicate sample of the uranyl carbonate solution used in the EXAFS experiments confirmed that the uranium was present as >97% [(UO$_2$)$_3$(CO$_3$)$_6$]$^{6-}$ both before and after data collection.

Crystallographic Studies. Large, needlelike crystals of **5** suitable for X-ray diffraction studies were grown from aqueous solution at 5 °C under an atmosphere of CO$_2$. The morphology of the crystals necessitated cutting, and X-ray photographs of several initial crystals showed broad peaks and indicated multiple crystal fragments. A small, irregular fragment measuring 0.15 × 0.2 × 0.2 mm was cut from a large needle, mounted on a glass fiber using silicon grease, and transfered to a Siemens R3m/V Diffractometer equiped with a low-temperature unit. Unit cell parameters were obtained by least squares refinement of 24 strong reflections well distributed in reciprocal space in the range of 20° < 2θ < 24°. Intensity data were collected at −44 °C using the ω scan technique with Mo Kα radiation under the condition given in Table 2.

The raw intensity data were corrected for background and Lorentz and polarization effects, and redundant data were merged. Atomic scattering factors and anomalous corrections were from the *International Tables for X-ray Crystallography*. Three check reflections measured every 100 reflections showed a 10% reduction in intensity during data collection, and a linear decay correction was applied to the data. An empirical absorption correction based on azimuthal (ψ) scans of three reflections located near χ = 90° was applied. The intensities were measured at 10° increments of rotation of the crystal about the diffraction vector, and the maximum and minimum transmission coefficients were 89% and 52%, respectively. The structure was solved by Patterson methods and refined by full-matrix least squares techniques using the SHELXTL PLUS suite of computer programs (Siemens Analytical X-ray Instruments, Inc., 1991).

The complex crystalizes in the triclinic space group $P\bar{1}$. Hydrogen atoms of the guanidinium cations were located and placed in fixed calculated positions, and their positional coordinates were constrained to "ride" on their parent atoms. The atoms of the anionic uranium trimer were refined with anisotropic temperature factors while the atoms of the guanidinium cations and the lattice waters were refined with isotropic temperature factors. One of the solvent water atoms, O(51), refined with an unreasonably large temperature factor and was therefore assigned a site occupancy factor of 0.5. Final refinement using 5482 unique, observed ($F > 3\sigma(F)$) reflections and 402 independent parameters converged to R = 0.0555, R_w = 0.0607 (where w = 1/[σ^2-$(F)^2+0.0004F^2$]), and GOF = 1.44. There is considerable residual electron density in the area of the uranium anionic complex with the largest peak , 4.0 e/Å^3, located 1.5 Å from U(1). Attempts to improve the model proved fruitless, and the relatively poor map is probably due to an inadequate empirical absorption correction.